

**Supplementary information**  
**Evolution of fluoride shuttle battery reactions and three-dimensional morphology changes of BiF<sub>3</sub> microparticles in an ethylene carbonate-based liquid electrolyte**

Toshiro Yamanaka,<sup>\*,a</sup> Zempachi Ogumi,<sup>a</sup> and Takeshi Abe<sup>b</sup>

*<sup>a</sup>Office of Society-Academia Collaboration for Innovation, Kyoto University, Katsura, Nishikyo, Kyoto 615-8530, Japan.*

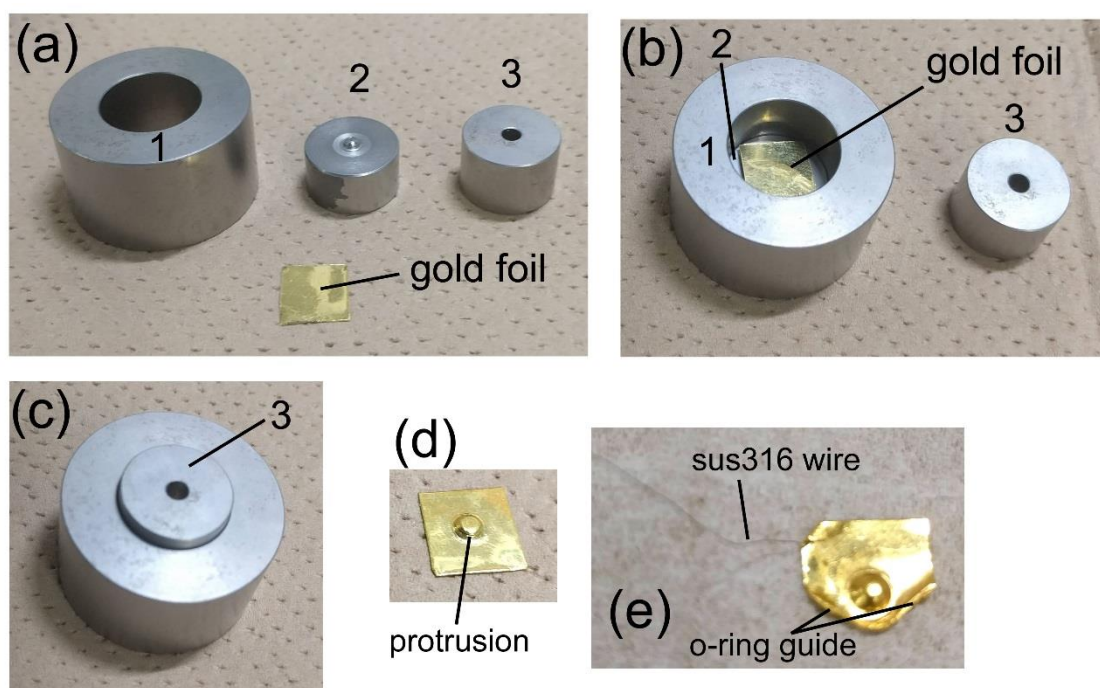
*<sup>b</sup>Graduate School of Global Environmental Studies, Kyoto University, Katsura, Nishikyo, Kyoto 615-8510, Japan*

\*e-mail: yamanaka.toshiro.8n@kyoto-u.ac.jp

## 1. Experimental details

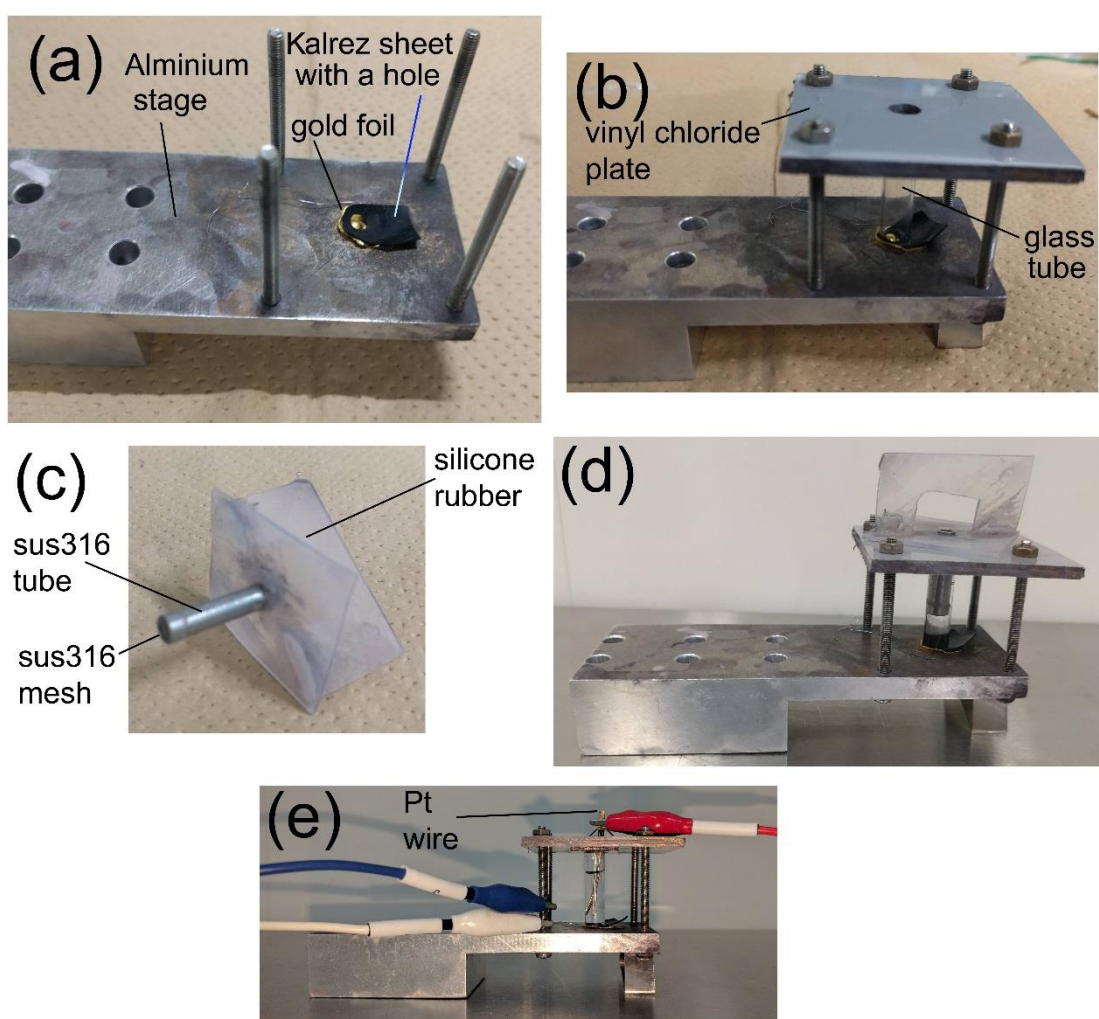
Since the amounts of o-BiF<sub>3</sub> in o-BiF<sub>3</sub> /gold and c-BiF<sub>3</sub> in c-BiF<sub>3</sub> /gold were very small, OCV was close to the potential of stainless steel, not the potentials of o-BiF<sub>3</sub> /gold and c-BiF<sub>3</sub> /gold, when o-BiF<sub>3</sub> /gold and c-BiF<sub>3</sub> /gold were supported by current collectors made of stainless steel. To obtain OCV values close to the potentials of o-BiF<sub>3</sub> /gold and c-BiF<sub>3</sub> /gold, the electrochemical Raman cell was made of only o-BiF<sub>3</sub> /gold and c-BiF<sub>3</sub> /gold, a kalrez o-ring, a Pb wire and a quartz window as follows, and stainless steel was not used.

Three pieces of stamp, 1-3 in Fig. S1a, were used to make a protrusion of a gold foil. The gold foil was pressed between 2 and 3 (Figs. S1b and S1c), resulting in a protrusion (Fig. S1d). Then the edge of the foil was bent (Fig. S1e), and the bent part was used as guides for the o-ring later. An SUS316 wire was spotwelded to the foil. (The wire was placed outside the cell later and it did not affect the OCV.)



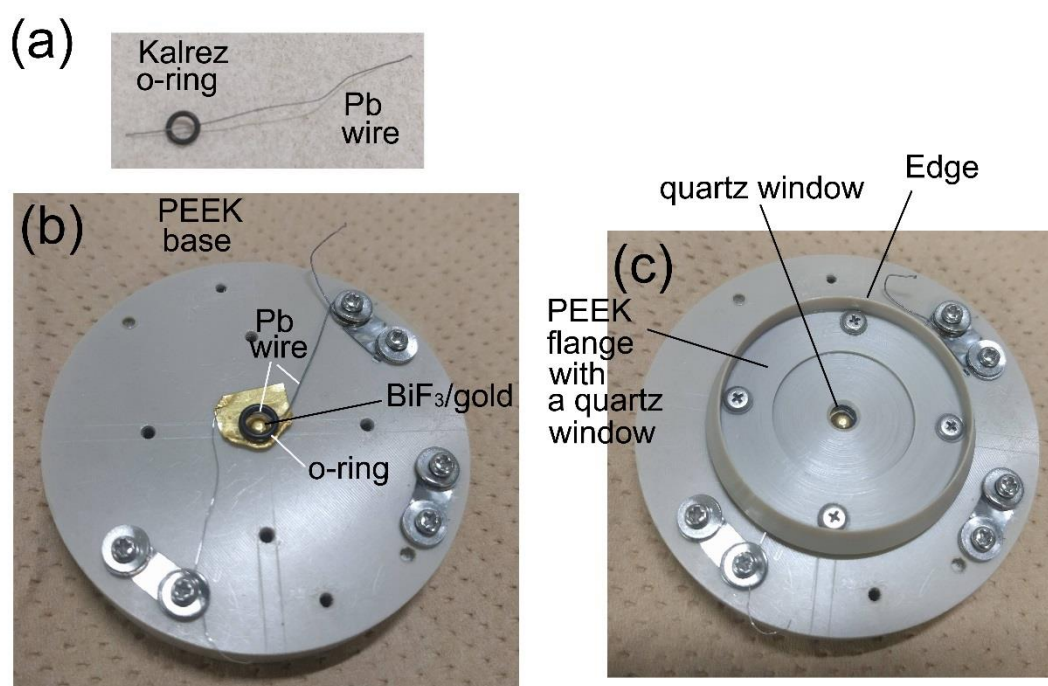
**Fig. S1** Processes of making a protrusion on a gold foil.

Figure S2 show the process of gold plating. The gold foil was put on an aluminium stage and a Kalrez sheet with a hole was put on it (Fig. S2a). Then a glass tube was pressed on the Kalrez sheet using a vinyl chloride plate with a hole (Fig. S 2b). The tube was filled with a gold plating solution, and a sieve made of sus316 (Fig. S2c) was inserted into the tube (Fig. S2d). Then o-BiF<sub>3</sub> or c-BiF<sub>3</sub> powder was put in the solution through the sieve. The sieve was taken off and a platinum wire was inserted. A current was applied between the platinum wire and the gold foil to make o-BiF<sub>3</sub> /gold and c-BiF<sub>3</sub> /gold (Fig. S2e).



**Fig. S2** Processes of gold plating to make o-BiF<sub>3</sub> /gold and c-BiF<sub>3</sub> /gold.

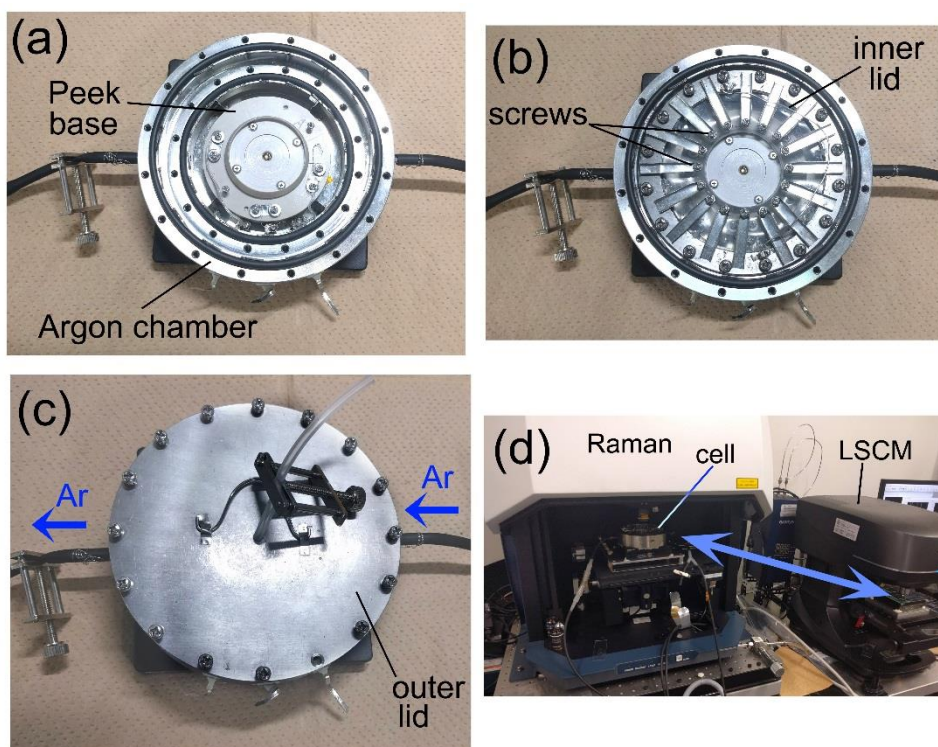
The electrochemical cell was assembled in an Ar atmosphere in a glove box. Figure S3 shows photographs of the processes of making the cell that were taken in air for explanation. A hole was made at the side of a Kalrez o-ring, and a Pb wire was inserted in the hole (Fig. S3a). The end of the Pb wire was polished to eliminate Pb oxide. o-BiF<sub>3</sub>/gold or c-BiF<sub>3</sub>/gold was put on a PEEK base and the o-ring was put on it (Fig. S3b). An electrolyte was dropped in the o-ring, and a PEEK flange with a quartz window was fixed on the o-ring using four screws (Fig. S3c). A piece of filter paper was inserted between the PEEK base and the PEEK flange to eliminate the excess electrolyte outside the o-ring.



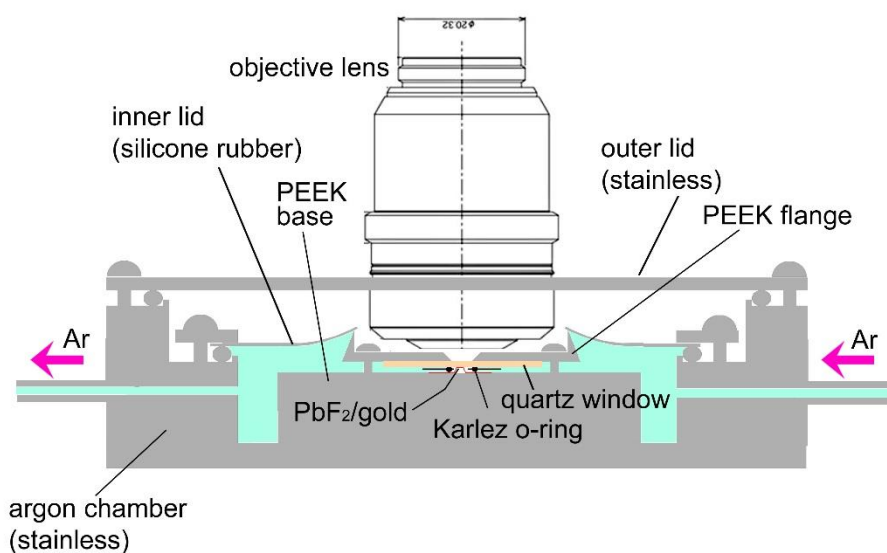
**Fig. S3** Processes of making an electrochemical Raman cell.

The PEEK base was put in an argon chamber (Fig. S4a) and the chamber was closed by an inner lid made of a silicone rubber sheet with a thickness of 0.5 mm (Fig. S4b). The sheet was gently pressed to the edge of the PEEK flange (Fig. S3c) and the degree of pressing was controlled by many screws (Fig. S4b). Then the chamber was strongly sealed by an outer lid. The argon chamber was taken off from the glove box and argon flow was started (Fig. S4c). Then the outer lid was taken off. Ar flowed below the inner lid and the PEEK flange (Fig. S5). Then the argon chamber with the cell was put on the sample stage of a Raman apparatus or an LSCM apparatus (Fig. S4d).





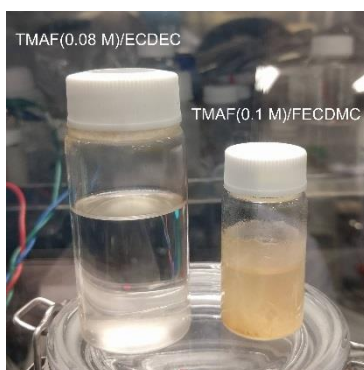
**Fig. S4** Starting Ar flow and setting of the cell on the stages of Raman and LSCM apparatuses.



**Fig. S5** Cross-sectional view of the argon chamber and the cell.

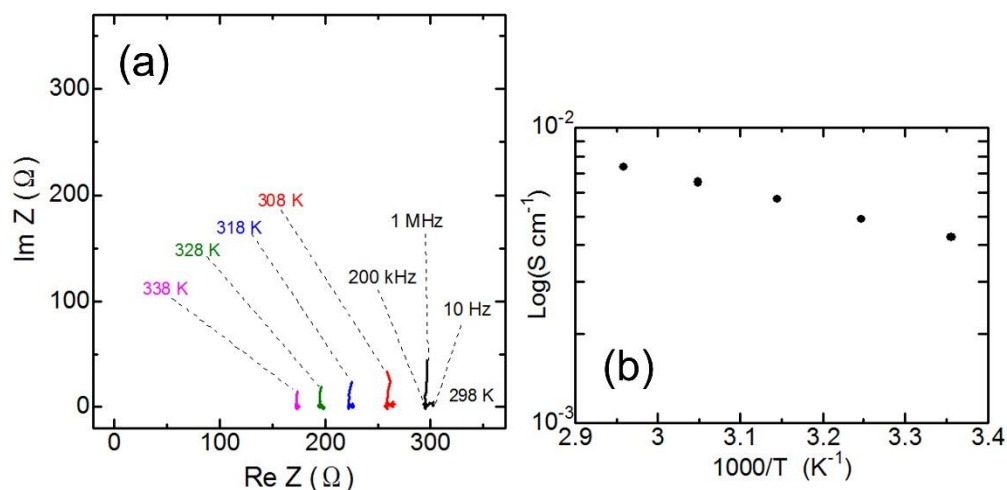
## 2. Ionic conductivity of the electrolyte

Figure S6 shows a photograph of the TMAF/ECDEC electrolyte after being kept in an Ar atmosphere for 10 months. The electrolyte is colorless and transparent. Degradation of the electrolyte was not recognized by its visual aspect. This is in contrast to a solution of TMAF (0.1 M) dissolved in a mixture of fluoroethylene carbonate (FEC) and dimethyl carbonate (DMC) (volume ratio of 1:1), which was colored when TMAF was dissolved in FECDMC.



**Fig. S6** photograph of the TMAF/ECDEC electrolyte and TMAF/FECDMC at 10 months after being prepared.

Figure S7a shows impedance spectra (1 MHz to 10 Hz) taken with a cell for the four terminal method (SB1400, EC frontier). The values of ionic conductivity derived from the spectra are shown in Fig. S7b.



**Fig. S7** Impedance spectra and values of ionic conductivity derived from the spectra.

### 3. Height profiles and starting positions of $F^-$ desorption from o-BiF<sub>3</sub> particles

The correlation between protrusions on the surfaces of o-BiF<sub>3</sub> particles and positions where desorption of  $F^-$  started (judged from the darkened contrasts) was further studied. Figures S8a and S3b show confocal CCD images of o-BiF<sub>3</sub>/gold at OCV and after  $E_{WE}$  was kept at 0.4 V for 6 hours. These images are the same as confocal CCD images shown in Figs. 3a and 3b in the main text. Figures S9a-S9k show height profiles along lines AB to lines UV in Fig. S8b, respectively. In Fig. S8b, contrasts of the positions indicated by white arrows became dark compared with those of corresponding positions in Fig. S8a. These positions correspond to the positions indicated by blue arrows in Figs. S9a-S9k, and there are protrusions at these positions. Thus, desorption of  $F^-$  is thought to start at protrusions.

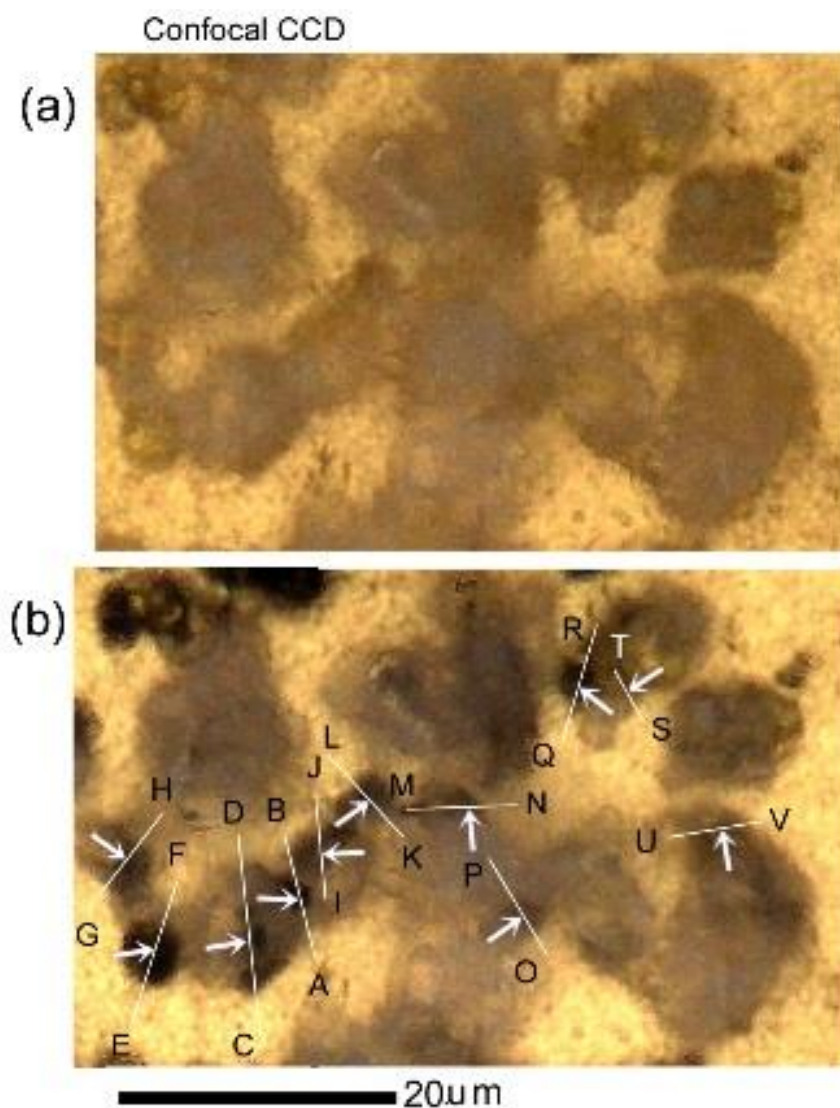


**Fig. S8** Confocal CCD images of o-BiF<sub>3</sub>/gold at OCV and after  $E_{WE}$  was kept at 0.4 V for 6 hours. These images are the same as confocal CCD images shown in Figs. 3a and 3b in

the main text. Height profiles along lines A-B to U-V are shown in Figs. S9a-S9k, respectively.

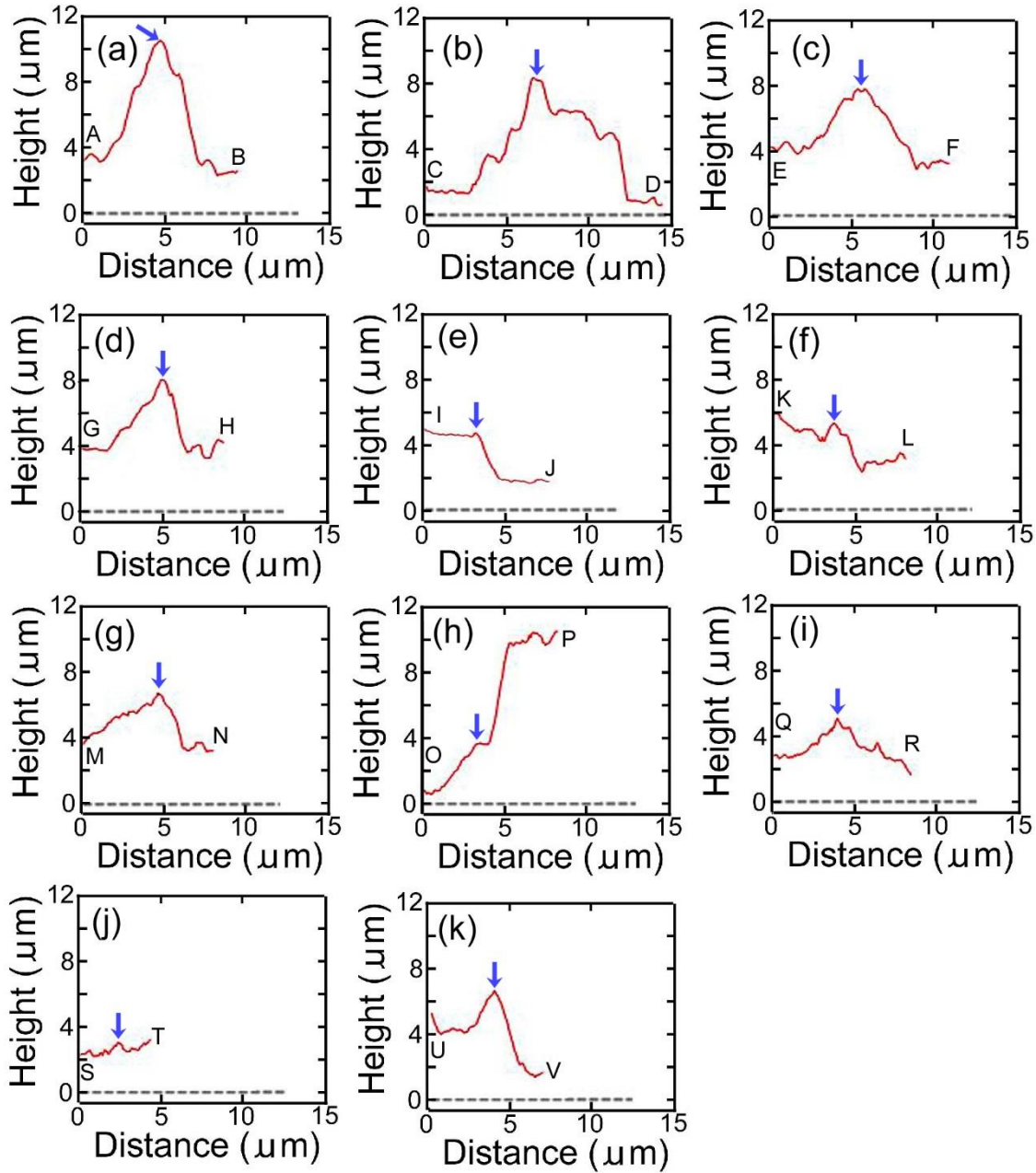


**Fig. S9** Height profiles along lines A-B to U-V in Figs. S8b. The positions indicated by blue arrows in (a)-(k) correspond to the positions indicated by white arrows on lines A-B to U-V, respectively.



#### 4. Height profiles and starting positions of F<sup>-</sup> desorption from c-BiF<sub>3</sub> particles

The correlation between protrusions on the surfaces of c-BiF<sub>3</sub> particles and positions where desorption of F<sup>-</sup> started (judged from appearance of the Raman peak of Bi) was studied. Figure S10a shows a confocal CCD image of c-BiF<sub>3</sub>/gold after E<sub>WE</sub> was kept at 0.4 V for 1.5 hours. The image is the same as that in Fig. 8a in the main text. Figure S10b shows superposition of a CCD image and Raman mapping for Bi after E<sub>WE</sub> was kept at 0.4 V for 1 hour. The superposition is the same as that in Fig. 7c in the main text. Height profiles along lines A-B to M-N are shown in Figs. S11a-S11g, respectively. The positions indicated by blue arrows correspond to those indicated by white arrows in Figs. S10a and S5b. In Fig. S10b, Bi appeared at positions close to white arrows. There are protrusions at the positions indicated by blue arrows in Figs. S11a-S11g. Thus, desorption of F<sup>-</sup> is thought to start at protruded positions.

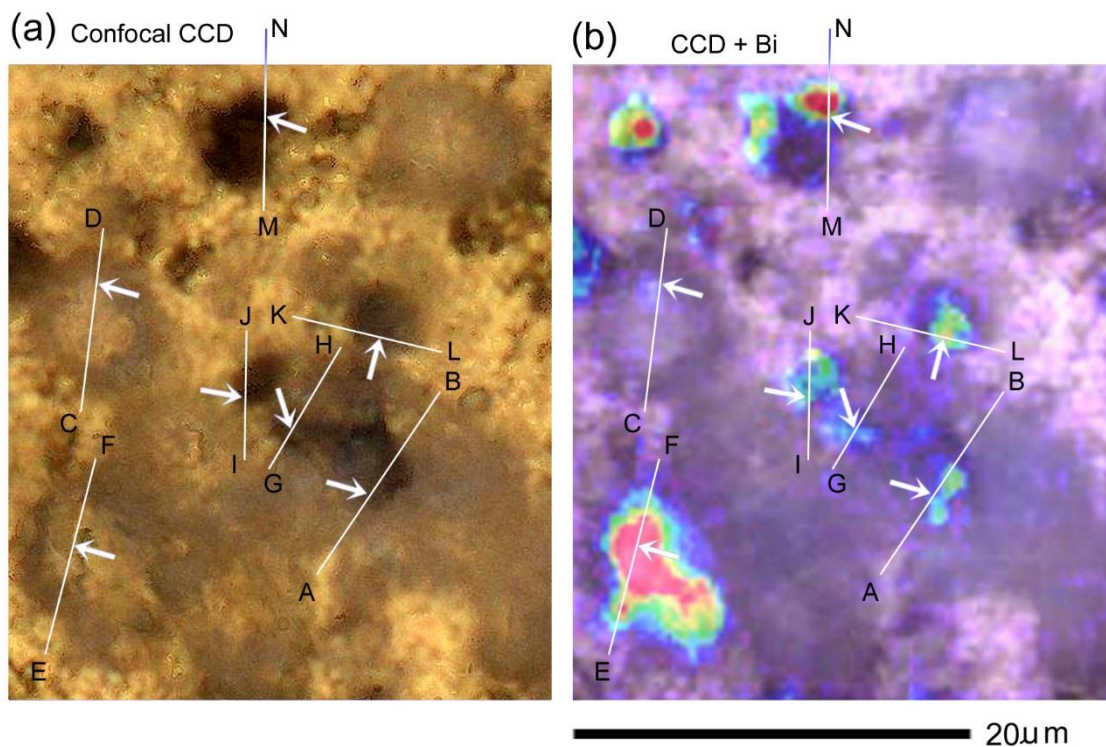


**Fig. S10** (a) Confocal CCD image of c-BiF<sub>3</sub>/gold after E<sub>WE</sub> was kept at 0.4 V for 1.5 hours. The image is the same as that in Fig. 8a in the main text. (b) Superposition of a CCD image of c-BiF<sub>3</sub>/gold and Raman mapping for Bi of c-BiF<sub>3</sub>/gold after E<sub>WE</sub> was kept at 0.4 V for 1 hour. The super position is the same as that in Fig. 7c in the main text.

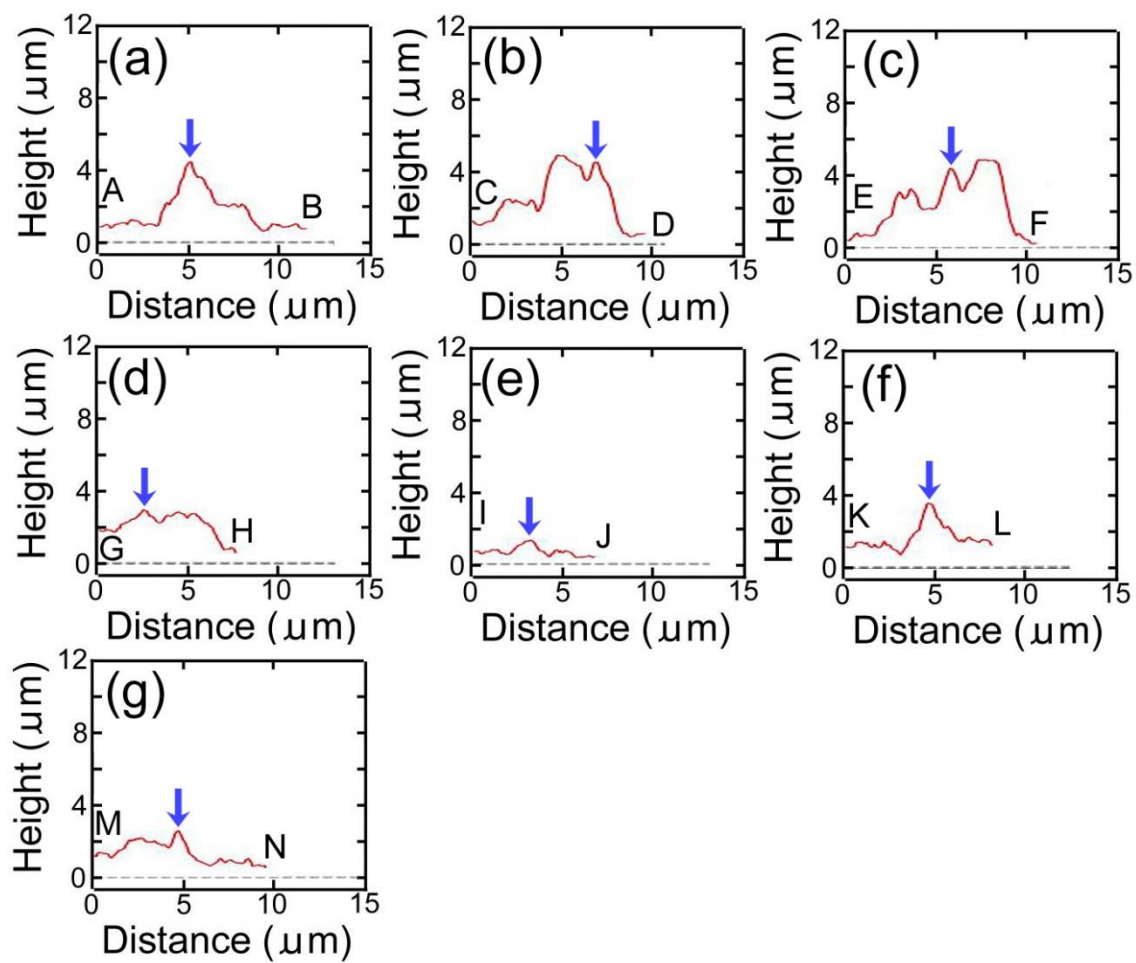


**Fig. S11** Height profiles along lines A-B to M-N in Figs. S10a and S10b. The positions indicated by blue arrows in (a)-(g) correspond to the positions indicated by white arrows on lines A-B to M-N, respectively.

## 5. CV measurements

Figure S12 shows results of cyclic voltammetry (CV) of the electrolyte taken with a glassy carbon electrode (working electrode), a platinum mesh (counter electrolyte), a silver rod (reference electrode) at a scan rate of 1 mV/s. The silver rod was immersed in acetonitrile with 0.1 M silver nitrate and 0.1 M tetraethylammonium perchlorate (0.587 V vs. standard hydrogen electrode (SHE)). At the 1<sup>st</sup> cycle, reduction started at -2.4 V and oxidation started at 0.5 V, resulting in a potential window from -2.4 V to 0.5 V. At the 4<sup>th</sup> cycle, reduction current around 3 V was partially suppressed. Oxidation above 0.5 V was also suppressed. Thus, the range of the potential window became wider. However, a significant reduction current was still observed below 3.2 V. The development of additives to make good SEI that effectively suppress reduction is needed, and it is expected that such additives will be developed in the future.

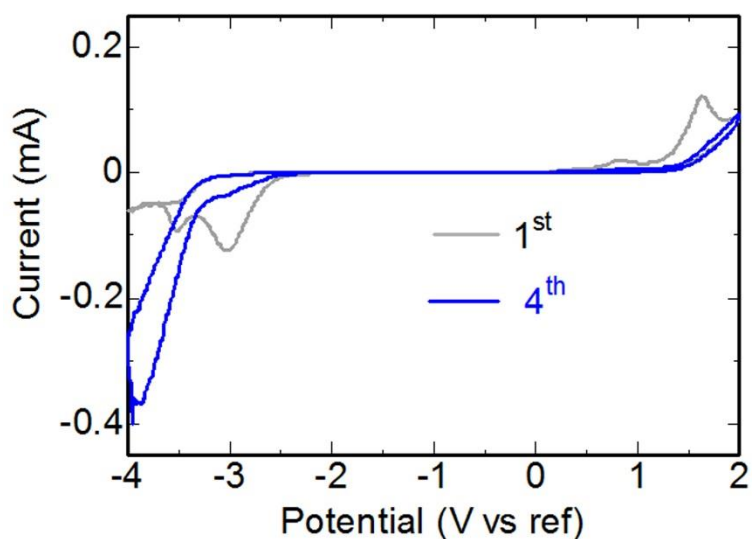


Fig. S12 Results of CV measurements of the TMAF/ECDEC electrolyte.